

Answers

Problem 1.

A non-linear least-squares problem was set up based on the sidebands.npz file data which contained a time-domain signal acquired during the measurement of the width of a resonance in an optical cavity via a laser with sidebands. Most of the laser power was located about a central frequency ν with deviation $\pm d\nu$. A piezo was utilized to mechanically push on the cavity, altering the resonant frequency thereof. The cavity resonant frequency was assumed to be shifted linearly in the time domain of interest.

a)

The data (signal magnitude of d v. time t) was modeled as a single Lorentzian, using analytic derivatives. Newton's method was utilized to carry out the fit. The Lorentzian was parametrized as follows:

$$d = a[1 + (t - t_0)^2/w^2]^{-1}.$$

The corresponding gradients were:

$$d_a = [1 + (t - t_0)^2/w^2]^{-1}.$$

$$d_w = 2aw(t - t_0)^2[(t - t_0)^2 + w^2]^{-2}.$$

$$d_{t_0} = 2aw^2(t - t_0)[(t - t_0)^2 + w^2]^{-2}.$$

The initial guesses for parameters amplitude a , width w , and center t_0 were $1.4 \cdot 10^{-5}$ and $2 \cdot 10^{-4}$, respectively.

The method matrix operations comprised $A_p^T N^{-1} A_p \delta p = A_p^T N^{-1} r$ where r is the residual difference between observed value of d and the predicted value $A(p_0)$.

After 10 iterations, the best-fit parameters for the amplitude a , width w , and center t_0 were identified as 1.423 , $1.792 \cdot 10^{-5}$, and $1.924 \cdot 10^{-4}$, respectively. Figure 1 shows the fitted Lorentzian compared to the raw data.

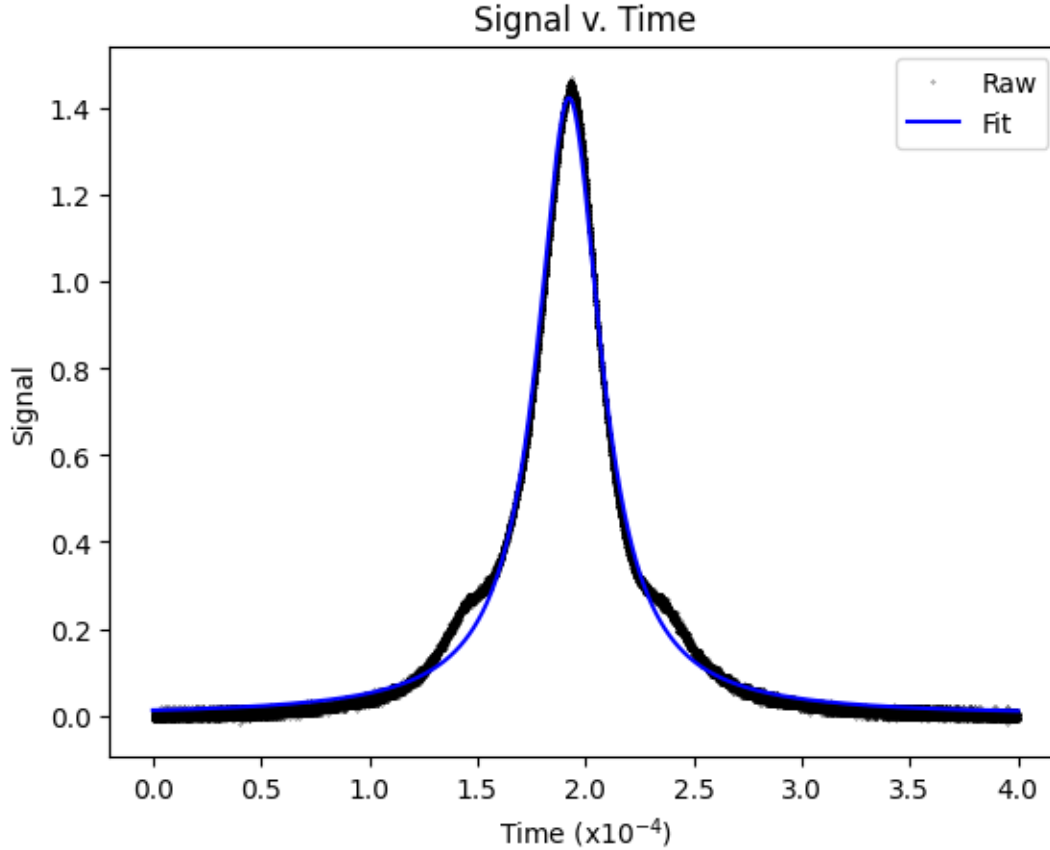


Figure 1. Comparison of Lorentzian fit with raw signal data

b)

The noise in the data was estimated based on a root mean square error analysis which could approximate the noise at 0.0252. Underlying premise was that this noise, which was uncorrelated, embodied the error in all observed points with a uniform distribution. The parameters with corresponding errors were computed as, amplitude a , width w , and center t_0 at $1.423 \pm 4.255 \times 10^{-4}$, $1.792 \times 10^{-5} \pm 7.588 \times 10^{-9}$, and $1.924 \times 10^{-4} \pm 5.358 \times 10^{-9}$, respectively.

c)

Part (a) was repeated with numerical derivatives. A helper function *numdiff* was constructed with an increment $h = (10^{-16})^{0.5} = 10^{-8}$ based on machine precision. The derivative f' was calculated as per the central difference method:

$$f' = [f(x+h) - f(x-h)]/(2h).$$

The resultant parameters with corresponding errors were computed as, amplitude a , width w , and center t_0 at $1.423 \pm 4.255 \times 10^{-4}$, $1.792 \times 10^{-5} \pm 7.588 \times 10^{-9}$, and $1.924 \times 10^{-4} \pm 5.358 \times 10^{-9}$, respectively. The parameters were not statistically significantly different from those calculated in part (a). Figure 2 shows that the fit based on a numerical derivative approach is near identical to that observed in Figure 1.

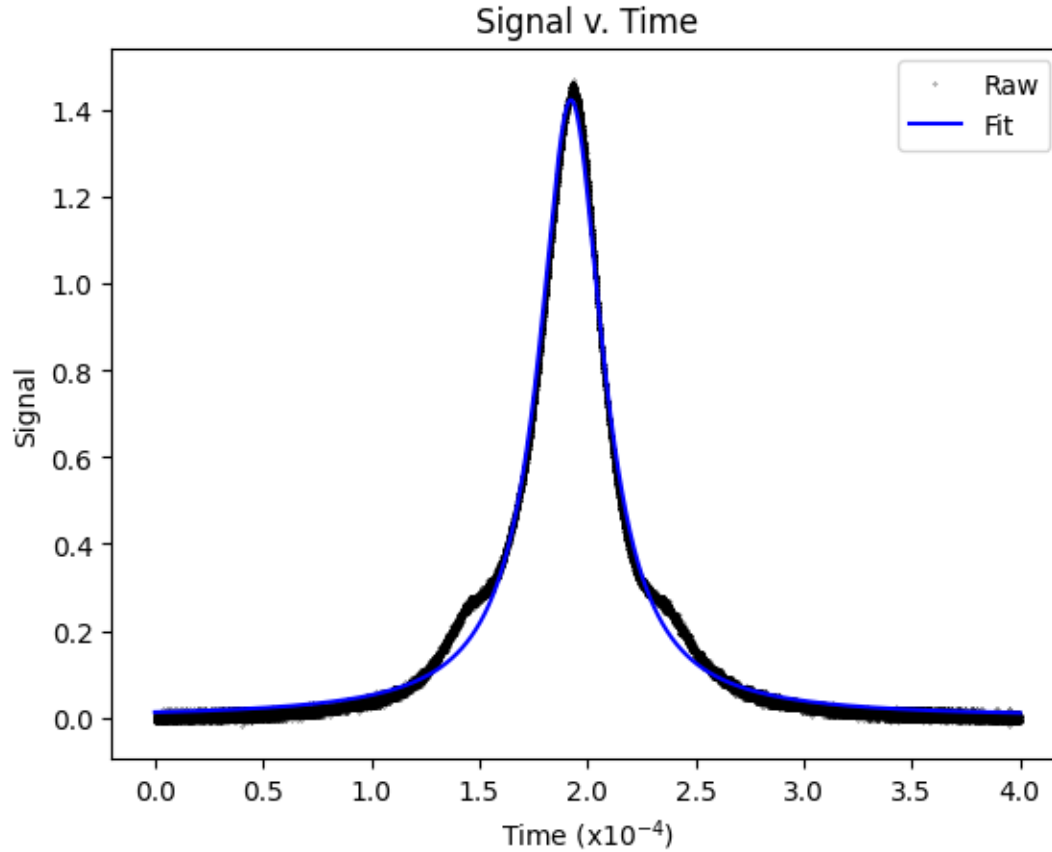


Figure 2. Comparison of Lorentzian fit with raw signal data (numerical derivative method)

d)

Part (c) was repeated with a new model comprising a sum of three Lorentzians. The width of all three Lorentzians would be the same, while the separation of the side peaks from the main peak should be equal. The new model was built according to:

$$d = a[1 + (t - t_0)^2/w^2]^{-1} + b[1 + (t - t_0 + dt)^2/w^2]^{-1} + c[1 + (t - t_0 - dt)^2/w^2]^{-1}$$

The initial guesses for parameters a , w , t_0 , b , c , and dt were 1.4, 1.7×10^{-5} , 2×10^{-4} , 1e-1, 1e-1, and 4×10^{-5} . After 10 iterations, the parameters with corresponding errors were calculated as follows:

$$\begin{aligned} a &= 1.443 \pm 2.664 \times 10^{-4} \\ w &= 1.607 \times 10^{-5} \pm 5.649 \times 10^{-9} \\ t_0 &= 1.926 \times 10^{-4} \pm 3.154 \times 10^{-9} \\ b &= 1.039 \times 10^{-1} \pm 2.541 \times 10^{-4} \\ c &= 6.473 \times 10^{-2} \pm 2.488 \times 10^{-4} \\ dt &= 4.457 \times 10^{-5} \pm 3.803 \times 10^{-8} \end{aligned}$$

Figure 3 shows the fitted new Lorentzian compared to the raw data.

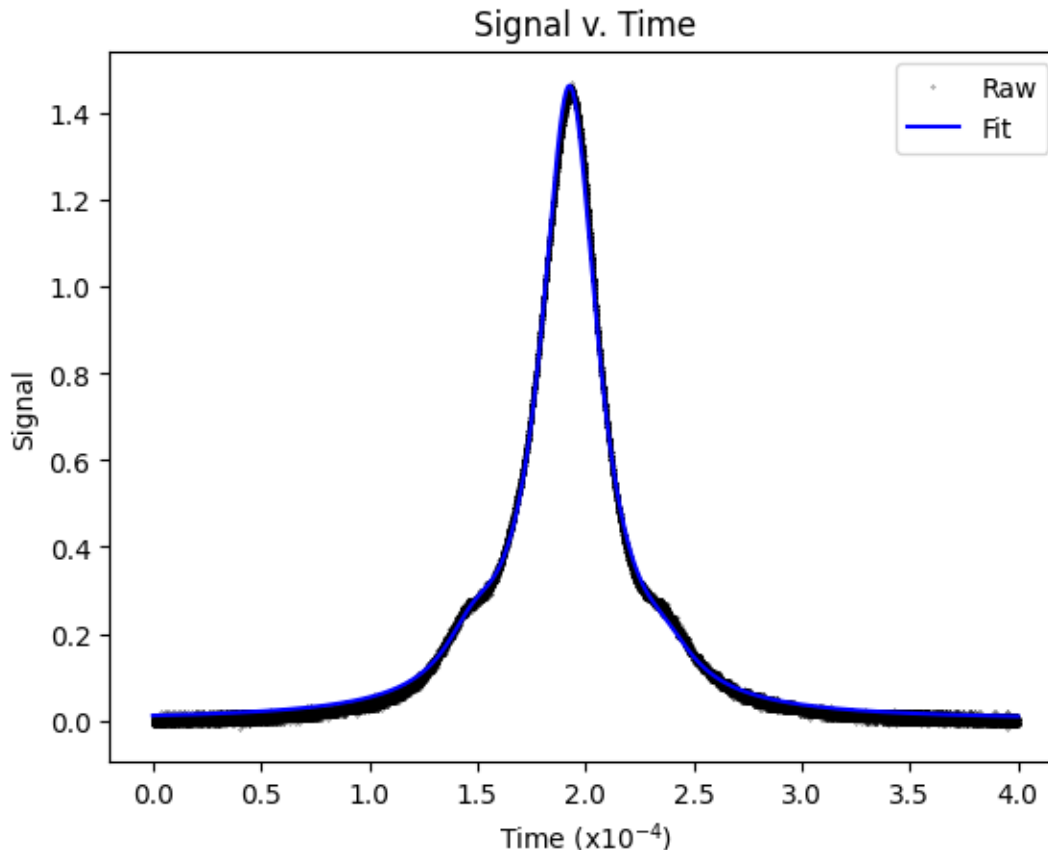


Figure 3. Comparison of new Lorentzian fit with raw signal data

e)

Residuals generated from subtracting the best-fit model in part (d) from the data were examined (Figure 4). An initial visual inspection of the residual profile revealed that the errors were not independent with uniform variance since there was an emerging pattern, roughly symmetrical about the midsection t_0 . Residuals were hence concluded to be not white. Thus, the new Lorentzian fit may not be a complete description of data and may benefit from further analysis to produce a better representative model to match the observed data, accounting for the correlation in the residuals.

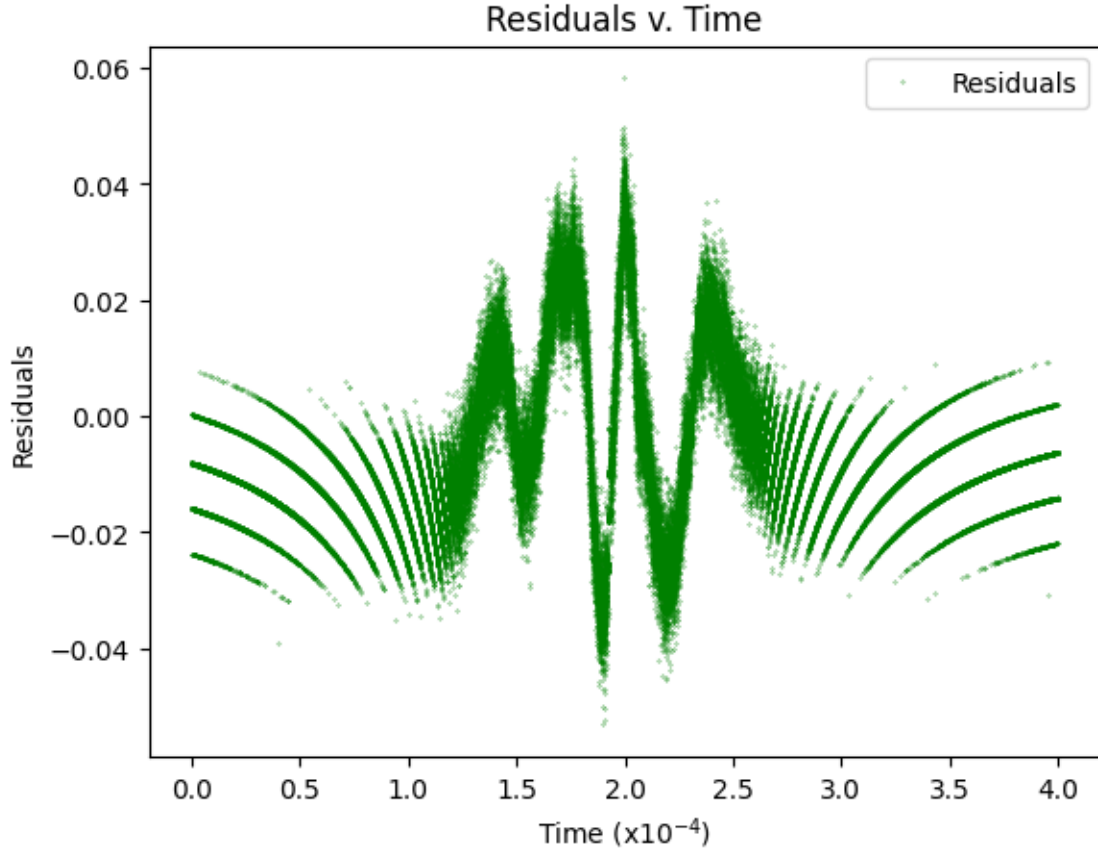


Figure 4. Residuals profile of new Lorentzian fit

f)

Four realizations for the parameter errors using the full covariance matrix $A^T N^{-1} A$ from part (d) were implemented. Cholesky decomposition facilitated generation of the add-on noise. The models constructed from adding these parameters to the parameter errors were plotted (Figure 5). The realizations were further examined as per their residuals (Figure 6). A chi-square analysis was carried out to compare the performance of the best-fit from part(d) to those of the four realizations. The χ^2 was defined as the sum of (observed – predicted)² for all data points.

The best-fit generated a $\chi^2 = 21.247$, while the four realizations exhibited χ^2 between 21.249 and 21.250. The best-fit χ^2 was slightly less than those in the range of realized χ^2 values. This trend is reasonable since the perturbances have caused the predictions to shift, albeit slightly, in the positive direction. Further analysis with 100 realizations were carried out, resulting in a mean $\chi^2 = 21.249$, which was in line with the observed χ^2 at four realizations.

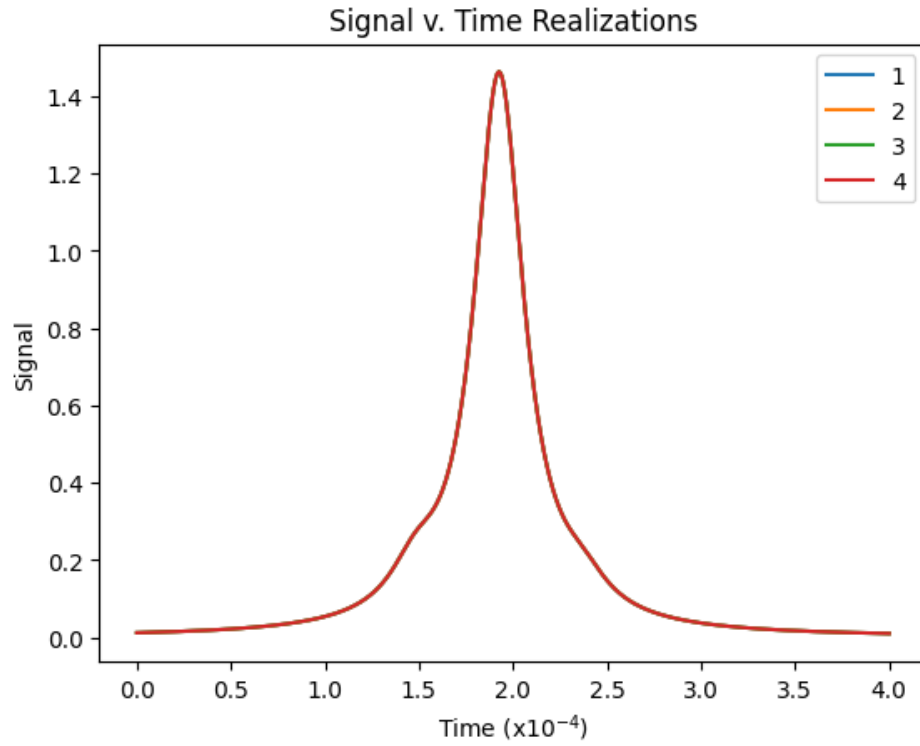


Figure 5. Four realizations of the parameter errors

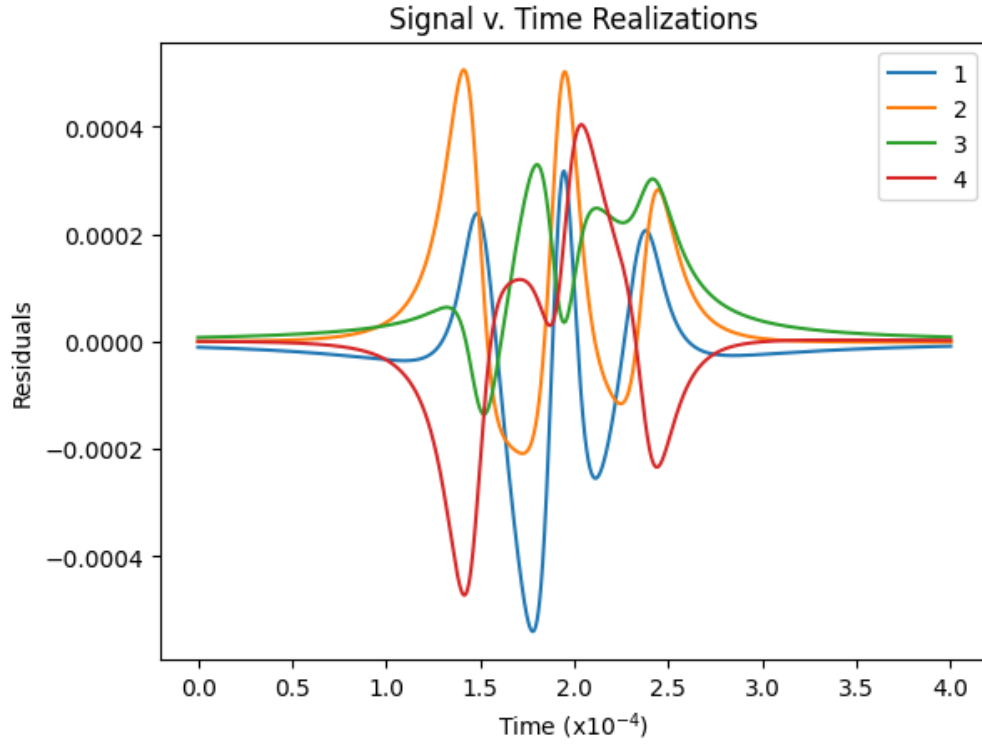


Figure 6. Residuals of four realizations of the parameter errors

g)

The fit from part (d) was redone, using an MCMC. The initial estimates were set as per the best fit parameter values from part (d), while the step-sizes were estimated according to the errors in the best fit parameter values. Figure 7 shows the behavior of each parameter along a chain index of 30000 length. The

According to Figure 7, all parameter plots produced for a chain revealed the presence of tight horizontal band across the history plots. In the absence of major fluctuations or jumps in the chain, the parameters may have been determined to have exhibited convergence.

The mean values of parameters with corresponding errors were calculated as follows:

$$a = 1.443 \pm 2.711 \times 10^{-4}$$

$$w = 1.606 \times 10^{-5} \pm 5.604 \times 10^{-9}$$

$$t_0 = 1.926 \times 10^{-4} \pm 3.261 \times 10^{-9}$$

$$b = 1.039 \times 10^{-1} \pm 2.501 \times 10^{-4}$$

$$c = 6.474 \times 10^{-2} \pm 2.432 \times 10^{-4}$$

$$dt = 4.457 \times 10^{-5} \pm 3.455 \times 10^{-8}$$

The errors were determined to be on the same order of magnitude as computed in part (d), thus in agreement with the best fit parameter values.

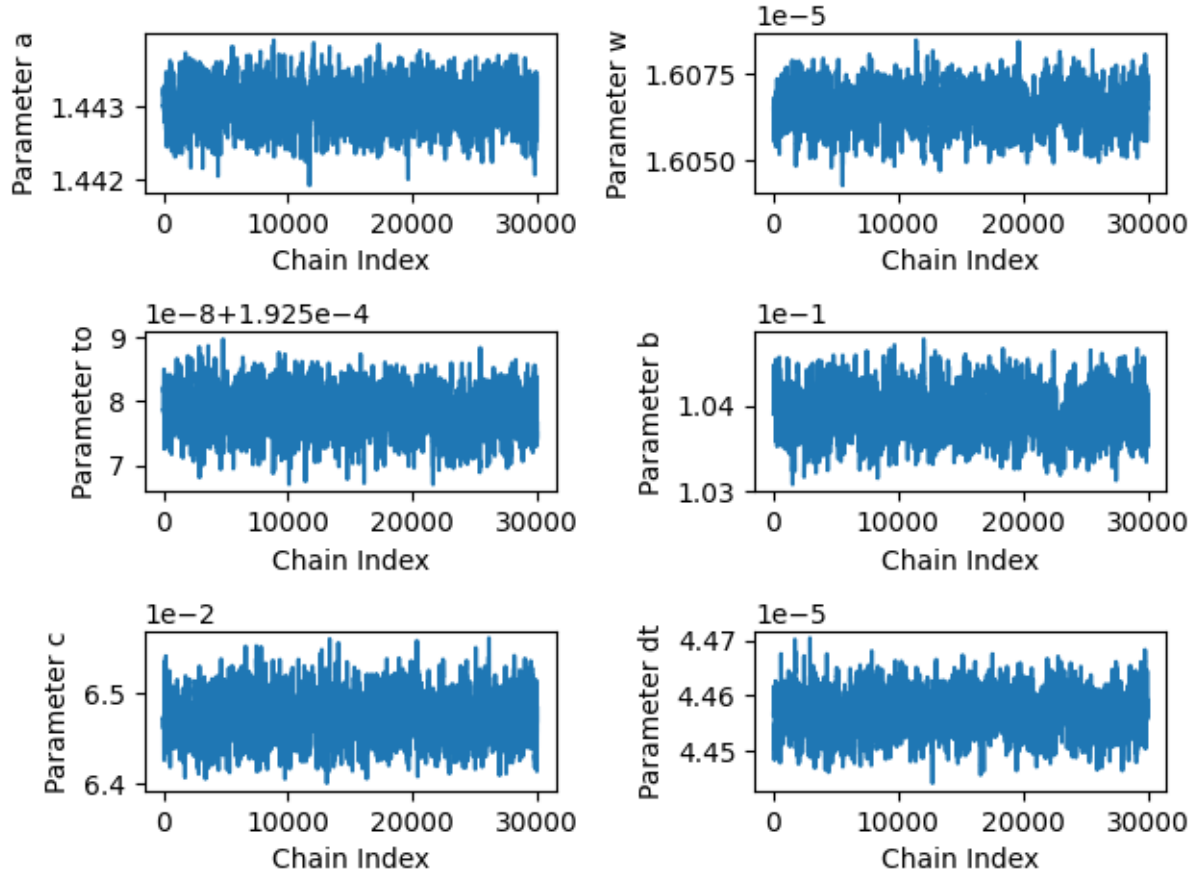


Figure 7. Parameter convergence in MCMC analysis

h)

Actual width of the cavity resonance in GHz was calculated based on dx mapped to 9 GHz. The mean values of w and dx from MCMC chains were computed. Subsequently, the cavity width could be found as follows:

width = 9 GHz (w/dx) where the error δ_{width} equalled $(\text{width})[(\delta_x/dx)^2 + (\delta_w/w)^2]^{1/2}$.

The width was determined to be 3.244 ± 0.003 GHz.

Appendix A: Python Code

Jupyter notebook with relevant Python code and outputs is available at:

https://github.com/ck22512/comp_phys/tree/main/Assignment4